

Modeling the austenite-ferrite transformation in microalloyed steel P510L

Wan-hua Yu¹, Lü-ting Xu¹, Guang-hong Feng², Chun-jing Wu¹, Cheng Zhou¹,
and Hui-feng Wang¹

1) School of Materials Science and Engineering, University of Science and Technology, Beijing 100083, China

2) Metallurgical Technology Institute, Central Iron and Steel Research Institute, Beijing 100081, China

(Received: 23 September 2009; revised: 20 October 2009; accepted: 28 October 2009)

Abstract: Based on experimental results, the transformation kinetics and cooling characteristics of low-carbon steel were analyzed and modeled to quantitatively link the operational parameters of a process with the properties. From the continuous cooling transformation results, comparisons of the start temperature of austenite-ferrite transformation among three models were analyzed, and the optimal $\ln k$ and n , which are the parameters in the Avrami equation, were determined by applying two regression models at different cooling rates. The transformation kinetics during continuous cooling was determined. Furthermore, reasonable agreements between experimental results and predictions were obtained, which can demonstrate the rationality of the established models.

Keywords: models; phase transformation; regression analysis; kinetics

1. Introduction

As a predicted tool to quantitatively link the operational parameters of a process with the properties, computer modeling is increasingly gaining significant attention. It is a challenge to develop an accurate mathematical model because of the complexity of thermal and mechanical properties of materials. Many researchers have made great efforts to these fields, and some achievements have been gained. However, the characteristics of the entire transformation process are not fully understood yet. Accelerated cooling on the run-out table is the final step before coiling, and it has been found that it has significant influence on the final microstructure and mechanical properties. On the run-out table, the main reaction is austenite-to-ferrite transformation ($\gamma \rightarrow \alpha$). The austenite-to-ferrite transformation of steels occurs in two steps: nucleation and growth. Upon nucleation, a new interface generates, which separates the product ferrite phase from the parent austenite phase. This interface migrates into the surrounding parent phase during the subsequent growth.

Aaronson and his co-workers made pioneering studies on the mechanism of ferrite nucleation in the condition of the

absence of retained strain, and it was believed that ferrite nucleated at austenite grain boundaries [1-4]. At present, there are several available models to describe the austenite-to-ferrite phase transformation, but it is argued that which one is better to describe the process. Militzer of the University of British Columbia (UBC) developed a series of models describing the phase transformation and properties since 1990s. Fifteen iron and steel companies in northern America developed an hot strip mill model (HSMM) based on the model proposed by Militzer [5-6]. Lee *et al.* proposed a multiple regression method and obtained $\ln k$ and n as a function of the chemical composition of steel and carbon content in untransformed austenite, which are the parameters in the Avrami equation. Trzaska and Dobrzanski [7] obtained k and n values in the Avrami equation for various phase transformations from the multiple regression method.

A new regression model was proposed in this paper, and it has good agreements between the experimental and predicted results through comparisons among the three models mentioned above. There are several methods to describe the transformation kinetics, such as JMAK equation, ISV framework, K-M equation, modified Zener-Hillert equation, modified Magee's rule, phase field model, the cellular

Corresponding author: Wan-hua Yu E-mail: ustbywh@sina.com

© University of Science and Technology Beijing and Springer-Verlag Berlin Heidelberg 2010

automaton method [8-9]. In this paper, the regression method with two models based on the Avrami equation to describe the transformation kinetics was employed.

2. Experimental

2.1. Materials

The chemical composition of the tested steel (P510L from Pangang Group Co. Ltd., China) is listed in Table 1.

Table 1. Chemical composition of P510L wt%

C	Si	Mn	P	S	V
0.080-	0.490-	0.930-	0.012-	0.007-	0.070-
0.110	0.590	1.060	0.023	0.012	0.080

2.2. Procedure

To determine the decomposition kinetics of austenite, dilatometric measurements were performed on the specimens (2 mm in diameter and 0.4 mm in thickness) using a DT-1000 thermal dilatometer. The dimension specification of the samples for it is shown in Fig. 1.

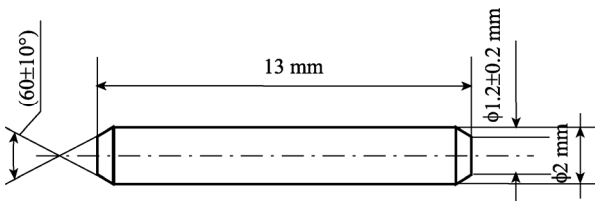


Fig. 1. Dimension specification of the samples for the DT-1000 dilatometer.

The samples were heated at 10°C/s to the austenizing temperature of 930°C, and held for 10 min to get a mean volumetric austenite grain size. Then the transformation test was performed by applying the appropriate cooling regime. The samples were cooled at the rates of 0.05, 0.1, 0.2, 2, 5, 10, 15, 21, 30, 35, 50, and 80°C/s, respectively, to room temperature, and dilatometry was employed to measure the austenite decomposition kinetics.

3. Results

The austenite-to-ferrite transformation was characterized by the expansion in the dilation measurement due to the change in the atomic volume of the phases produced to determine the transformation kinetics [10]. Fig. 2 shows an expansion curve at a cooling rate of 0.05°C/s. Assuming that the length change of the sample is proportional to the volume fraction of phase transformation, the graphic method in Fig. 2 can be employed to determine the temperature with a

certain transformation fraction. Corresponding temperatures for the different volume fractions of phase transformation are gained at 0.05, 0.2, and 5°C/s as shown in Table 2.

Fig. 3 shows an example of austenite decomposition kinetics vs. the temperature of P510L steel at various cooling

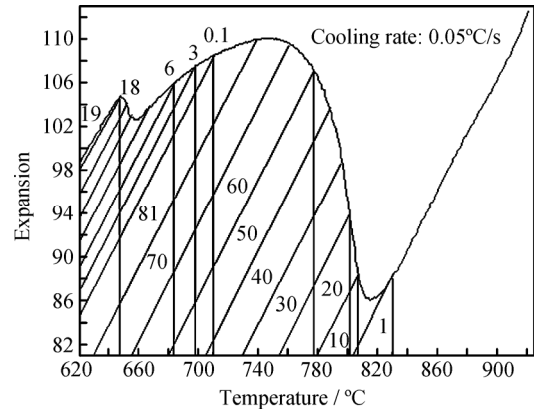


Fig. 2. Expansion chart for the different volume fractions (vol%) of phase transformation.

Table 2. Temperatures for the different volume fractions of phase transformation at different cooling rates

Volume fraction	Cooling rate / (°C·s ⁻¹)		
	5.0	0.2	1.0
0.01	775.0	809.0	775.0
0.10	755.0	792.6	755.0
0.20	748.0	787.0	748.0
0.30	743.0	783.6	743.0
0.40	736.0	775.5	736.0
0.50	729.0	764.6	729.0
0.60	720.0	750.0	721.0
0.70	705.0	728.6	705.0
0.80	685.0	707.8	685.0
0.91	651.5	687.0	651.5

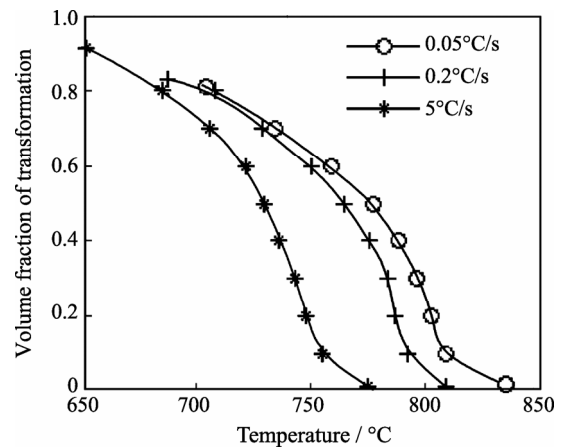


Fig. 3. Transformation kinetics for the P510L steel obtained from the continuous cooling testing (CCT) tests.

rates, obtaining from the expansion curve by an equal division method. The start temperatures of the austenite-to-ferrite transformation at different cooling rates are obtained from the test as shown in Table 3.

The CCT diagram and metallographs of P510L show that the final microstructure is predominantly block ferrite and a few pearlite which appears at the ferrite grain boundary at 0.2°C/s, as illustrated in Fig. 4(a). In Figs. 4(b)-(c), the mixed structures of ferrite and pearlite are obtained at 5 and 10°C/s, and more pearlite is found with the increase of cooling rate. A small amount of lateral flake Widmanstätten structure is observed in Fig. 4(c). The final microstructure is

the mixed structures of ferrite, pearlite, and bainite at 21°C/s as shown in Fig. 4(d). Since bainite in Fig. 4(d) is difficult to recognize, the scan electric microscopy (SEM) photograph is adopted to prove the existence of bainite, as illustrated in Fig. 5(a). The amount of bainite increases, and ferrite decreases gradually with the increase of cooling rate, even part of austenite transforms to bainite directly. As shown in Figs. 4(e)-(f), the microstructure is predominantly ferrite and lath bainite for the cooling rates of 35 and 80°C/s. Fig. 5(b) is the SEM photograph at 35°C/s. Because of the restriction of experimental condition, the highest cooling rate adopted is 80°C/s, and no martensite is observed.

Table 3. Start temperature of the austenite-to-ferrite transformation (T_s) at different cooling rates of P510L

Steel No.	12	11	01	02	03	04	05	06	07	08	09	10
Cooling rate / (°C·s ⁻¹)	80	50	35	30	21	15	10	5	2	0.2	0.1	0.05
T_s / °C	722	736	744	751	783	752	772	776	798	830	844	832

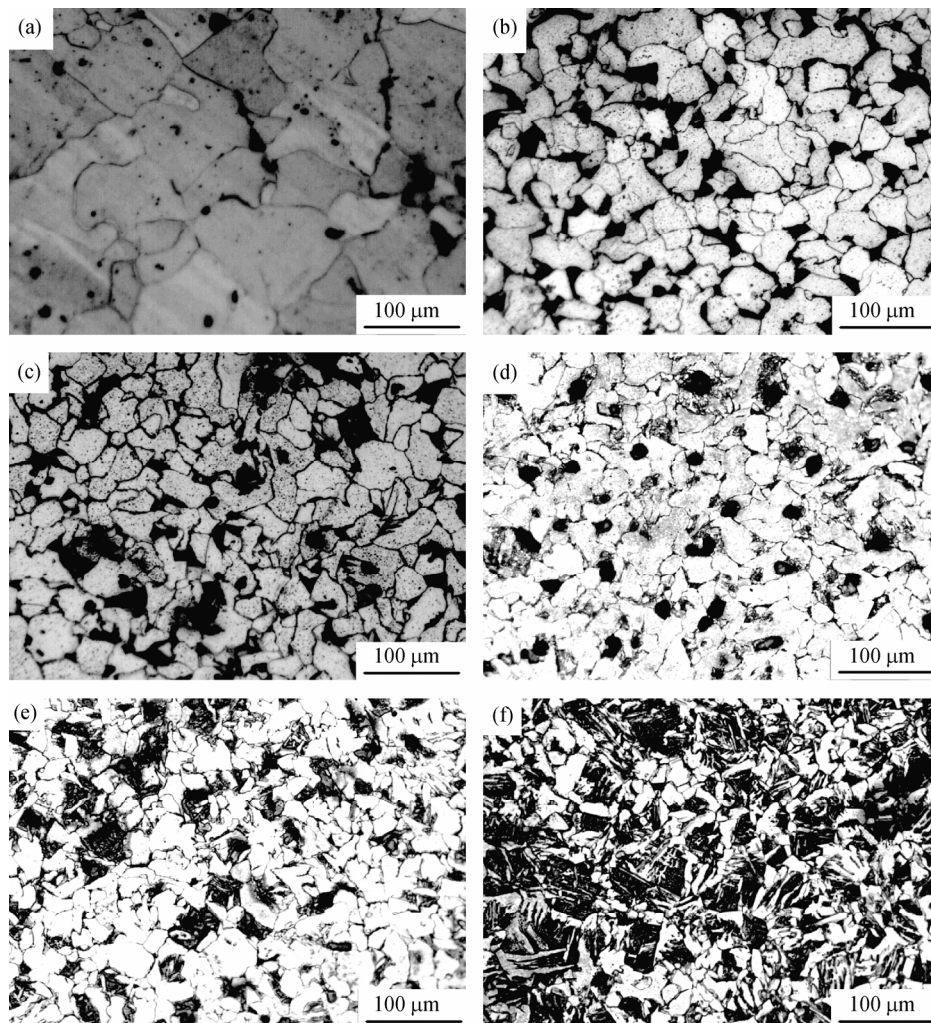


Fig. 4. Final microstructures obtained at different cooling rates: (a) 0.2°C/s; (b) 5°C/s; (c) 10°C/s; (d) 21°C/s; (e) 35°C/s; (f) 80°C/s.

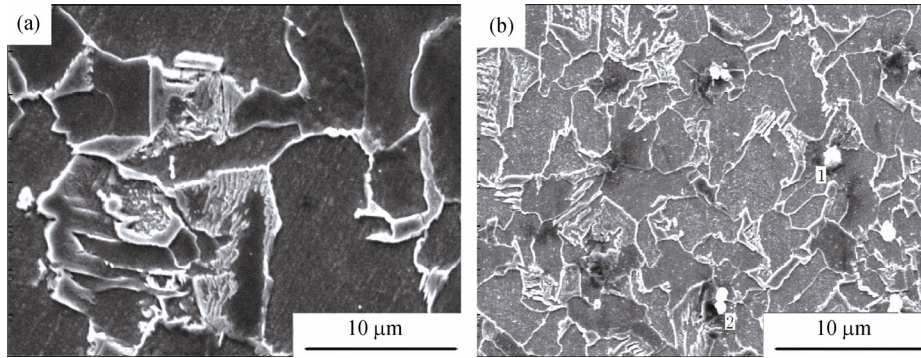


Fig. 5. SEM photographs of different cooling rates: (a) 21°C/s; (b) 35°C/s.

4. Modeling the start temperature of austenite-to-ferrite transformation

4.1. Model a

This model was proposed by Militzer [5-6]. The early growth of corner nucleated ferrite is assumed to be controlled by carbon diffusion in austenite. The growth rate can be considered as the steady-state parabolic growth.

$$\frac{dR}{dt} = D_c \frac{c_\gamma - c^0}{c_\gamma - c_\alpha} \frac{1}{R} \quad (1)$$

where R is the radius of the corner nucleated ferrite grain, D_c the carbon diffusion coefficient, c^0 the carbon bulk concentration, and c_γ and c_α are the equilibrium carbon concentrations in austenite and ferrite, respectively. For the start temperature of austenite to ferrite transformation (T_s) is reached when

$$R \frac{c_\gamma - c^0}{c_* - c_\alpha} = \frac{d_\gamma}{\sqrt{2.1}} \quad (2)$$

where d_γ is the volumetric austenite grain size, and c_* the limiting concentration, above which nucleation is inhibited [5].

$$c_* = 1.3c^0 \text{ (Plain carbon steel),}$$

$$c_* = 1.4c^0 \text{ (High strength low alloy (HSLA) grades).}$$

Fig. 6 shows a comparison between experimental data and predicted values with the model of Militzer. It can be seen that good agreement is obtained at higher cooling rates; however, the predicted values at lower cooling rates are lower than experimental results. Nucleation temperature for ferrite in the model of Militzer (T_N) is probably the key to the problem. The decision of T_N is a complicated process

which involves many parameters [6]. The classical nucleation rate (J) can be expressed as

$$J = \eta \frac{2D\Omega x}{a^4 (3kT)^{1/2}} \exp\left(-\frac{\zeta}{\Delta G^2 kT}\right) \quad (3)$$

where ΔG is the driving force for ferrite nucleation, D the relevant diffusivity of the rate-determining species with an atomic fraction x , Ω the atomic volume of ferrite, a the average lattice parameter of ferrite and austenite, k the Boltzmann's constant, T the temperature, and η and ζ are the parameters which depend on the potential nucleation site density and interfacial energies, respectively. Enomoto and Aaronson carefully investigated ferrite nucleation at austenite grain boundaries and found that ferrite nucleation occurred only at a few preferred sites at the boundaries. They also favored the composition and a pillbox shape of the nuclei. Within the coherent pillbox model,

$$\eta = N(\gamma_c + \gamma_0 - \gamma_{gh})^{1/2} \quad (4)$$

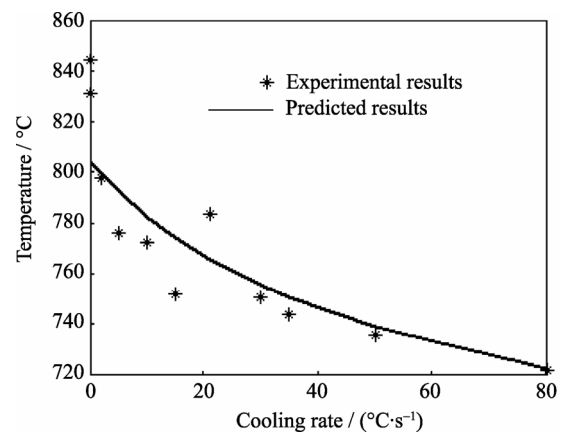


Fig. 6. Comparison between experimental results and predictions for the start temperature of austenite-to-ferrite transformation at different cooling rates with model a.

and

$$\zeta = 4\pi\gamma_e^2(\gamma_c + \gamma_0 - \gamma_{gh}) \quad (5)$$

where γ_{gh} is the grain boundary energy, γ_e the interfacial energy of the various partially or fully coherent surfaces, γ_0 the facet energy in the grain boundary plane, γ_c the facet energy with upper grains, and N the number of grains.

The nucleation temperature (T_N) obtained during continuous cooling can be determined by

$$\Theta = \int_{T_N}^{T_{Ae3}} \frac{J(T)}{\phi(T)} dT \quad (6)$$

where T_{Ae3} is the start temperature of austenite deposition in equilibrium conditions, ϕ the cooling rate, and Θ the critical nucleation density evaluated from the number of ferrite grains nucleated per austenite grain (M) by the following equation:

$$M = F \left(\frac{d_\gamma}{d_\alpha} \right)^3 \quad (7)$$

where F is the ferrite volume fraction, d_γ the austenite grain size, and d_α the ferrite grain size. For the simplicity of the model, a temperature of 40°C lower than T_{Ae3} is empirically employed as T_N . This may probably cause the deviation

between predicted start temperatures and experimental ones at lower cooling rates.

4.2. Model b

The method of multiple regressions was used to model the start temperature of austenite-to-ferrite transformation which was developed by Trzaska and Dobrzanski. The start temperature of the austenite-to-ferrite transformation (T_s) is calculated as [7]

$$T_s = a_0 - a_1 \cdot C - a_2 \cdot Mn + a_3 \cdot Si - a_4 \cdot Cr - a_5 \cdot Ni - a_6 \cdot Mo + a_7 \cdot V - a_8 \cdot T_A - a_9 \cdot v_\gamma^{a_{10}} \quad (8)$$

where T_A is the temperature at Ae3 line in the phase diagram, v_γ the cooling rate before the phase transformation, and the values of coefficients a_0 - a_{10} obtained from multiple regressions are listed in Table 4. The following equation can be obtained:

$$T_s = 968.7 - 254C - 71Mn + 27.6Si - 30Cr - 44Ni - 54Mo + 95.8V - 0.02T_A - 62.8v_\gamma^{0.25} \quad (9)$$

According to the results obtained from the experiment, it is reasonable to modify the regression value a_{10} to 0.18 as illustrated in Fig. 7. Good agreement between the measured transformation behaviors and calculated ones is obtained except that at the cooling rate of 21°C/s.

Table 4. Values of regression coefficients

a_0	a_1	a_2	a_3	a_4	a_5	a_6	a_7	a_8	a_9	a_{10}
968.70	254.00	71.00	27.60	30.00	44.00	54.00	95.80	0.02	62.80	0.25

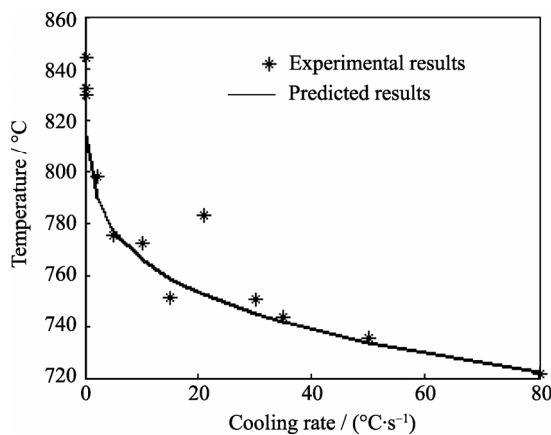


Fig. 7. Comparison of experimental results and predictions for the start temperature of austenite-to-ferrite transformation at different cooling rates with model b.

4.3. Model c

An equation to model the phase transformation in the process of austenite decomposition during continuous cooling is established to describe the relationship between start temperature and cooling rate [10].

$$T_s = T_{Ae3} - AV^B \quad (10)$$

where V is the cooling rate, A and B are the regression coefficients. T_s can be gained through the regression of coefficients A and B . The start temperature of austenite decomposition to ferrite, pearlite, bainite, and martensite can be calculated with the equation, respectively. According to the experimental data given in Table 2, the following equation is obtained through employing a nonlinear regression method:

$$T_s = T_{Ae3} - 31.9189V^{0.3071} \quad (11)$$

The comparison of experimental results and predictions by Eq. (11) for the start temperature of austenite-to-ferrite transformation at different cooling rates are shown in Fig. 8. It can be seen that a reasonable agreement between two sides is obtained.

Comparisons among three models that describe the start temperatures of austenite-to-ferrite at different cooling rates are carried out in Fig. 9. Model a has its own restrictions because of the complicated process of T_N decision. The reasonable agreements between experimental results and predictions are obtained both from models b and c. However, since ten coefficients of regression are required for the decision of the model b equation, it has no advantage in the aspect of simplicity comparing to model c, for which only two regression coefficients are needed.

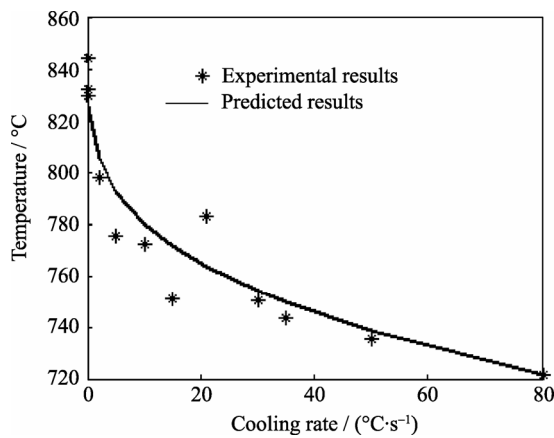


Fig. 8. Comparison of experimental results and predictions for the start temperature of austenite-to-ferrite transformation at different cooling rates with model c.

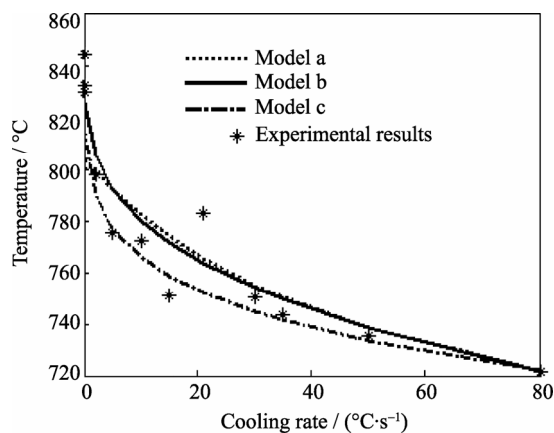


Fig. 9. Comparisons of experimental results and predictions for the start temperature of austenite-to-ferrite transformation at different cooling rates with three models.

5. Regression of phase transformation kinetics

Many researchers have generalized the transformation behavior of steel through the experimental examination and mathematical modeling. It is well established that the non-isothermal transformation behavior can be described by the additive rules. The isothermal decomposition of austenite is represented by the Avrami equation.

$$X / X_e = 1 - \exp(-kt^n) \quad (12)$$

where X is the volume fraction of the transformed phase after transformation time t ; X_e the thermodynamic equilibrium volume fraction of ferrite, which can be determined from the equilibrium phase diagram with the given temperature and chemical composition; k the rate constant, which depends on the temperature and transformation mechanism; and n the time exponent, which is a constant over the temperature range when a unique transformation mechanism operates.

The isothermal transformation behavior can be characterized by kinetic parameters, k and n , from the Avrami plot of the transformation curve. By rearranging Eq. (12), the following equation is obtained:

$$\ln \left\{ \ln \left[1 / (1 - X / X_e) \right] \right\} = \ln k + n \ln t \quad (13)$$

The values of k and n can be determined from the intercept and slope of the $\ln \{ \ln [1 / (1 - X / X_e)] \}$ vs. $\ln t$ plot.

In this paper, a regression method was used with the experimental results given in Table 3 to determine $\ln k$ and n . Two regression models for model c are established as follows.

$$\text{Model c-1: } \ln k = A + B \ln(T_{Ae3} - T) + \frac{C}{T} \quad (14)$$

$$\text{Model c-2: } \ln k = AT^2 + BT + C \quad (15)$$

Umemoto modified Chan's model for the austenite-to-ferrite transformation behavior based on the parabolic diffusional growth of ferrite nuclei. In his report, he showed that the time exponent (n) would be 1/2, 1, and 3/2 for each cases of face, edge, and corner nucleation, respectively, when the nucleation site was saturated immediately at the beginning of transformation.

It is interesting to note that the time exponent (n) represents the dimensionality of diffusional growth under the site saturation condition. For the case of grain face nucleation, the extended volume increases in one-dimensional growth

of nuclei to the direction normal to the face, because the growth of nuclei to the direction parallel to the face is blocked by neighbor nuclei. Similarly, the extended volume increases in two-dimensional growth of nuclei to the direction normal to the edge for the case of grain edge nucleation, and the extended volume increases in three-dimensional growth of nuclei to the direction normal to the corner for the case of grain corner nucleation.

The early stage of austenite-to-ferrite transformation kinetics is governed by the two-dimensional growth of nuclei saturated at the grain edge. However, as the radius of ferrite grains increases, another restriction of ferrite grains is expected due to neighbor austenite grain edges. This implies that the two-dimensional growth at the early stage of transformation will be changed to one-dimensional growth as the transformation proceeds. Thus, the time exponent (n) of the Avrami equation for isothermal austenite-to-ferrite transformation should not be a constant but a function of transformed fraction as the following [11-12]:

$$X / X_e = 1 - \exp[-kt^{f(X)}] \quad (16)$$

$$n = f(X) = 1 - 0.5X^2 \quad (17)$$

When the two regression models are employed, $\ln k$ is decided in condition that n is fixed at 0.5, 1, 1.5, and $1-0.5X^2$.

The optimal value of $\ln k$ is obtained from the regression with Eq. 14 as follows, when n is 0.5, 1, 1.5, and $1-0.5X^2$, respectively.

$$\ln k = 2.8588 + 2.7809 \ln(T_{Ae3} - T) - \frac{1.3824 \times 10^4}{T} \quad (18)$$

$$\ln k = 2.1537 + 2.0777 \ln(T_{Ae3} - T) - \frac{1.3827 \times 10^4}{T} \quad (19)$$

$$\ln k = 1.1870 + 1.3751 \ln(T_{Ae3} - T) - \frac{1.3830 \times 10^4}{T} \quad (20)$$

$$\ln k = -11.9437 + 2.8449 \ln(T_{Ae3} - T) - \frac{4.6351 \times 10^3}{T} \quad (21)$$

Comparisons of the T - $\ln k$ relationship between the experimental and regression results with Eq. 14 at 0.05°C/s are carried out in Fig. 10. It can be seen that good agreement between the experimental T - $\ln k$ relationship and regression results is reached when $n=1-0.5X^2$.

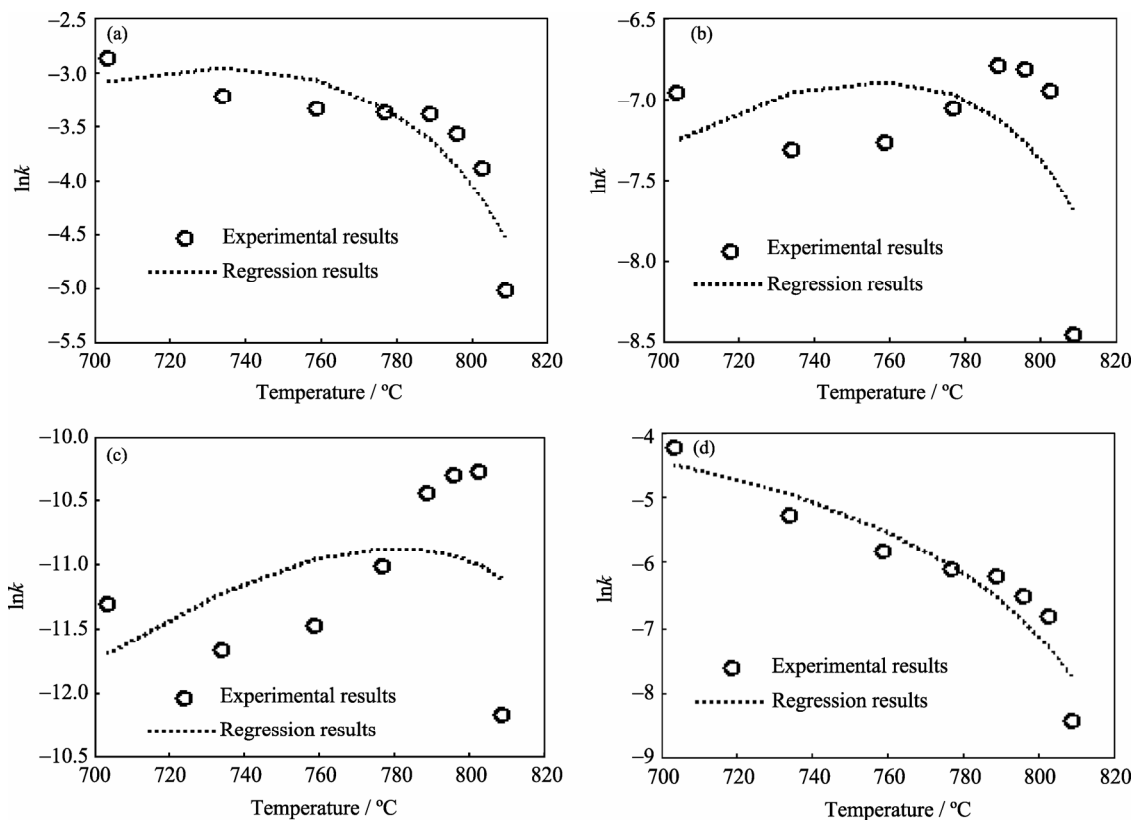


Fig. 10. Comparisons of the experimental T - $\ln k$ relationship with regression results in model c-1 with different n values: (a) $n=0.5$; (b) $n=1$; (c) $n=1.5$; (d) $n=1-0.5X^2$.

The optimal value of $\ln k$ is obtained from the regression with Eq. 15 as follows, when n is 0.5, 1, 1.5, and $1-0.5X^2$, respectively.

$$\ln k = -2.2618 \times 10^{-4} T^2 + 0.3298 T - 123.1317 \quad (22)$$

$$\ln k = -1.3918 \times 10^{-4} T^2 + 0.2074 T - 84.2049 \quad (23)$$

$$\ln k = -5.2170 \times 10^{-5} T^2 + 0.085 T - 45.5397 \quad (24)$$

$$\ln k = -1.9480 \times 10^{-4} T^2 + 0.2653 T - 94.7086 \quad (25)$$

Comparisons of the T - $\ln k$ relationship between the experimental and regression results of Eq. 15 at 0.05°C/s are carried out in Fig. 11. Good agreement between the experimental T - $\ln k$ relationship and regression results is reached when $n=1-0.5X^2$.

The following optimal n and $\ln k$ for $\gamma \rightarrow \alpha$ transformation can be obtained with the method described above. An example of comparison between the measured transformation behaviors and calculated ones which are obtained from the

regression of $\ln k$ by the Avrami Equation and Schiel additivity is shown in Fig. 12. The calculated results are in reasonable agreement with the experimental data.

6. Conclusions

(1) Comparisons among three models that describe the start temperature of austenite-to-ferrite transformation at different cooling rates are carried out, and it is concluded that model a has its own restrictions because of the complicated process of T_N determination. Reasonable agreements between the experimental results and predictions are obtained both from model b and model c. However, the determination of model b equations requires ten regression coefficients, so it has no advantage in the aspect of simplicity comparing to model c, which just needs two regression coefficients.

(2) From the continuous cooling data, optimal $\ln k$ and n are obtained from two regression models at different cooling rates. The transformation kinetics during continuous cooling is determined. Reasonable agreements between experimental results and predictions are obtained.

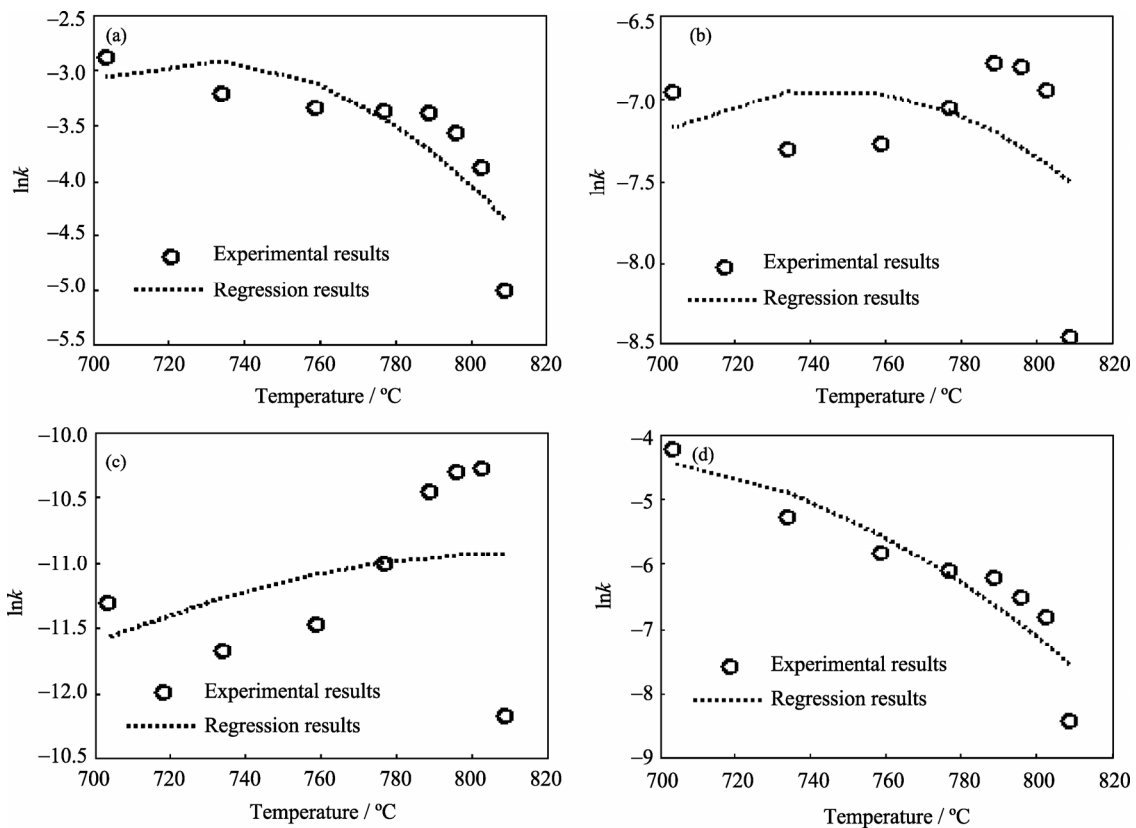


Fig. 11. Comparisons of the experimental T - $\ln k$ relationship with regression results in model c-2 with different n values: (a) $n=0.5$; (b) $n=1$; (c) $n=1.5$; (d) $n=1-0.5X^2$.

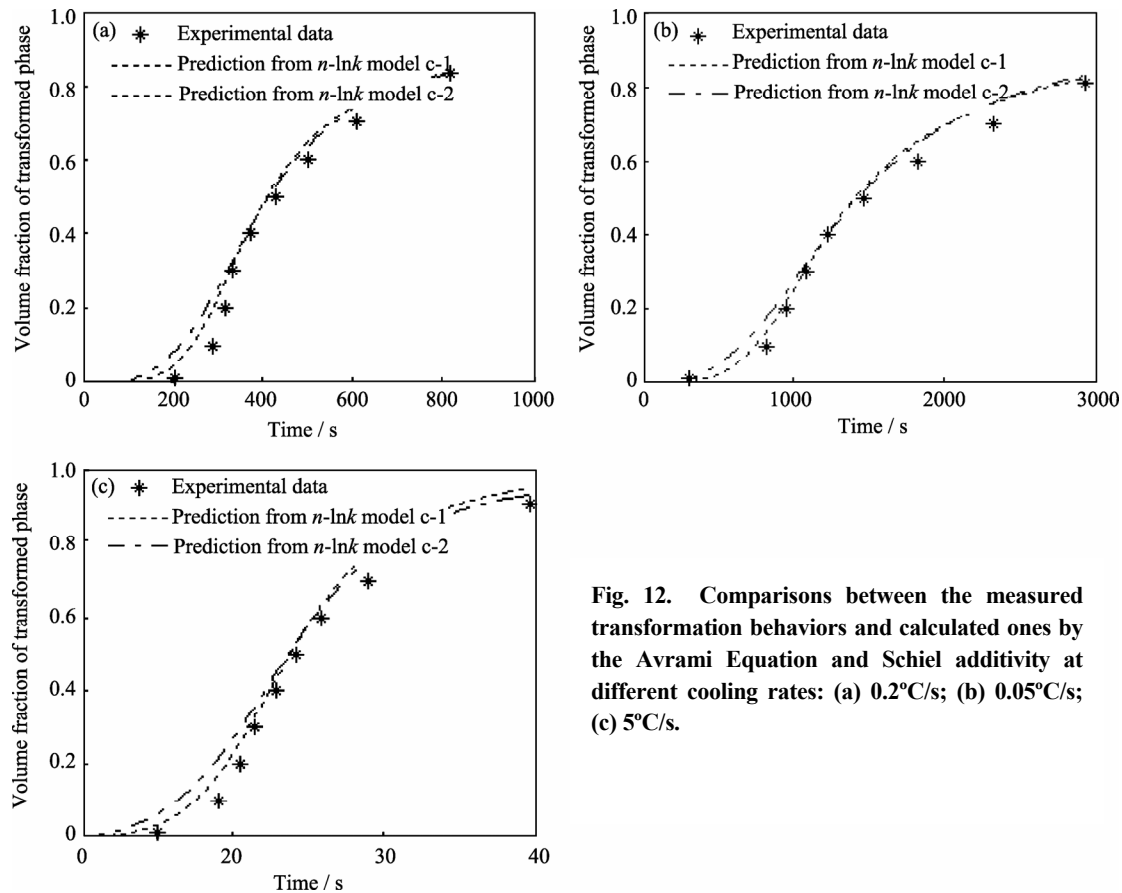


Fig. 12. Comparisons between the measured transformation behaviors and calculated ones by the Avrami Equation and Schiel additivity at different cooling rates: (a) 0.2°C/s; (b) 0.05°C/s; (c) 5°C/s.

Acknowledgement

The authors appreciate the financial support of Pangang Group Co. Ltd., China.

References

- [1] M. Enomoto and H.I. Aaronson, On the critical nucleus composition of ferrite in an Fe-C-X alloy, *Metall. Trans. A*, 17(1986), No.5, p.1381.
- [2] M. Enomoto and H.I. Aaronson, Nucleation kinetics of proeutectoid ferrite at austenite grain boundaries in Fe-C-X alloys, *Metall. Trans. A*, 17(1986), No.5, p.1385.
- [3] M. Enomoto, W.F. Aaronson, and H.I. Aaronson, The kinetics of ferrite nucleation at austenite grain edges in Fe-C and Fe-C-X alloys, *Metall. Trans. A*, 17(1986), No.8, p.1399.
- [4] W.F. Lange, M. Enomoto, and H.I. Aaronson, The kinetics of ferrite nucleation at austenite grain boundaries in Fe-C alloys, *Metall. Trans. A*, 19(1988), No.6, p.427.
- [5] M. Militzer, R. Pandi, E.B. Hawbolt, and T.R. Meadowcroft, Modelling the phase transformation kinetics in low-carbon steels, [in] H.J. McQueen, E.V. Konopleva, and N.D. Ryan, eds., *Hot Workability of Steels and Light Alloys-Composites*, CIM, Montreal, 1996, p.373.
- [6] M. Militzer, R. Pandi, and E.B. Hawbolt, Ferrite nucleation and growth during continuous cooling, *Metall. Trans. A*, 27(1996), No.8, p.1547.
- [7] J. Trzaska and L.A. Dobrzański, Modelling of CCT diagrams for engineering and constructional steels, *J. Mater. Process. Technol.*, 192(2007), No.5, p.504.
- [8] H.Z. Zhao, X.H. Liu, and G.D. Wang, Progress in modeling of phase transformation kinetics, *J. Iron Steel Res. Int.*, 13(2006), No.3, p.68.
- [9] Y.T. Zhang, D.Z. Li, and Y.Y. Li, Modelling of austenite decomposition in plain carbon steels during hot rolling, *J. Mater. Process. Technol.*, 171(2006), p.175.
- [10] A. Kumar, C. McCulloch, E.B. Hawbolt, et al., Modelling thermal and microstructural evolution on runout table of hot strip mill, *Mater. Sci. Technol.*, 7(1991), p.360.
- [11] E.B. Hawbolt, B. Chau, and J.K. Brimacombe, Kinetics of austenite-ferrite and austenite-pearlite transformations in a 1025 carbon steel, *Metall. Trans. A*, 16(1985), p.565.
- [12] J.K. Lee and H.N. Han, Mathematical modeling of transformation and cooling behaviors of high carbon steels on run-out table of hot strip mill, [in] *Thermomechanical Processing of Steels*, London, 1998, p.245.